Green Chemistry

PAPER

View Article Online
View Journal | View Issue

Cite this: *Green Chem.*, 2020, **22**, 6531

The production of valuable biopolymer precursors from fructose†

Xuan Liu, Daniel Chee Yin Leong and Yujie Sun *

Received 7th July 2020,
Accepted 11th September 2020

DOI: 10.1039/d0gc02315a

rsc.li/greenchem

The increasing demand for green chemical products calls for the exploration of sustainable and renewable carbon resources beyond fossil-based materials, whose utilization inevitably results in environmental concerns. As such, biomass valorisation has attracted increasing attention because biomass is the most widely available and sustainable carbon source. Among the available biomass-derived platform chemicals, 5-hydroxymethylfurfural (HMF) has long been regarded as an attractive candidate for the production of numerous value-added products. Nevertheless, the poor stability, and difficult separation and purification of HMF from fructose dehydration significantly inhibit its large-scale application. Herein, we report a two-step process for the direct production of two biopolymer precursors, 2,5-furandicarboxylic acid (FDCA) and 2,5-bis(hydroxymethyl)furan (BHMF), from fructose, bypassing the isolation of HMF. FDCA and BHMF are much easier to separate and purify from the reaction mixture than HMF, and they both can replace petroleum-based counterparts in the syntheses of many industrially important polymers, ranging from polyesters to polyamides. Optimized fructose dehydration under microwave irradiation achieved a high HMF yield (83%) using a biphasic strategy. The subsequent electrocatalytic conversion of the resulting microwave reaction mixture allowed us to carry out either oxidation or reduction *via* readily tuning the electrochemical parameters to yield FDCA or BHMF, respectively. The integration of microwave irradiation and electrocatalysis in a flow electrolyzer enabled the direct conversion of readily available fructose to highly valuable FDCA and BHMF without the expensive and challenging step of HMF isolation, suggesting an economically attractive approach for upgrading carbohydrates.

1. Introduction

The long-term and detrimental consequences of climate change resulting from continued utilization of fossil reserves inspire the exploration of alternative carbon resources together with innovative technologies for the conversion of renewable and sustainable carbon to fuels, chemicals, and materials. Within this context, biomass refinery has attracted increasing attention in the past two decades, particularly in the upgrading of biomass-derived feedstocks to value-added products.[1,2] One of those products from C6 carbohydrates is 5-hydroxymethylfurfural (HMF), which has been referred to as a "sleeping giant" of sustainable chemistry and can act as a platform compound for the syntheses of numerous commodity chemicals, polymers, plastics, pharmaceuticals, and liquid fuels.[3,4] For instance, its oxidation product, 2,5-furandicarboxylic acid (FDCA), is a green replacement of terephthalic acid to produce polyamides, polyesters, and polyurethanes.[5–10] On the other hand, its reduction product, 2,5-bis(hydroxymethyl)furan (BHMF), can also be used as a precursor for the synthesis of important renewable biopolymers.

HMF oxidation to produce FDCA has been extensively studied in both homogeneous and heterogeneous catalysis.[11,12] Moderate yields of FDCA (60–80%) could be achieved using inexpensive homogeneous catalysts like Co $(OAc)_2$ and Mn$(OAc)_2$ at high temperature and under high O_2 pressure,[13] albeit subsequent treatment is required to purify FDCA and recover the catalysts, raising additional energy and capital cost. In contrast, relatively higher FDCA yields could be obtained with heterogeneous catalysts; however, most of them consist of noble metals such as Pt, Pd, and Au.[14,15] With the aim of substantially decreasing the energy input and financial investment, electrocatalytic oxidation of HMF to FDCA in aqueous media under ambient conditions has emerged as a very promising strategy. Indeed, many research groups, including ours, have been devoted to designing and developing various low-cost electrocatalytic systems, most of which are solely composed of earth-abundant elements, for the electrocatalytic production of FDCA from HMF oxidation.[16–18]

A similar scenario can be drawn for the reductive transformation (hydrogenation) of HMF to BHMF. Conventional

Department of Chemistry, University of Cincinnati, Cincinnati, OH 45221, USA. E-mail: yujie.sun@uc.edu

†Electronic supplementary information (ESI) available. See DOI: 10.1039/d0gc02315a

thermocatalysis is typically conducted under harsh conditions, such as high temperature and high pressure (8–65 bar), using H_2 as the hydrogen source in the presence of heterogeneous catalysts, such as Pt, Ir, and Au.[19,20] Apparently, H_2 itself is a high-cost hydrogen source, and such a HMF hydrogenation step usually exhibits low H_2 utilization.[21–23] Parallel to the growing interest in the electrocatalytic oxidation of HMF, electrocatalytic hydrogenation has very recently attracted attention as a green and inexpensive method for converting HMF to BHMF, although the electrochemical reduction of ketones and aldehydes to alcohols has been known for decades.[24,25] To date, Pd and Ag have been identified as particularly effective for the electrocatalytic hydrogenation of HMF to BHMF in aqueous electrolytes, utilizing water as the hydrogen source.[26–29]

Owing to the large amount of demand for HMF, a significant amount of effort has been devoted to developing effective means for HMF production, among which a common strategy is fructose dehydration (Table 1). For instance, Riisager *et al.* reported the microwave-assisted dehydration of fructose catalyzed by HCl in water at 200 °C, and an HMF yield of 53% was obtained (entry 1). However, side reactions, such as polycondensation and rehydration of HMF, are also favoured in pure aqueous media.[30] In order to minimize side reactions, organic solvents, including dimethylacetamide (DMA, entry 2), dimethyl sulfoxide (DMSO, entry 3), and formic acid (entry 4), have been found to exhibit decent HMF yields, ranging from 73% to 93%.[31,32] However, a much longer reaction time (>2 h) was required. Furthermore, the high boiling points of these organic solvents also render the downstream separation difficult. More recently, Dumesic and co-workers reported the effectiveness of biphasic solvents, such as γ-valerolactone (GVL) and water, for fructose dehydration, with HMF yields of 70% (entry 5) and 78% (entry 6).[33,34] It was rationalized that biphasic media would favor the extraction of HMF from the aqueous phase to the organic phase and limit the formation of by-products like humins. When the starting concentration of fructose was as low as 1 wt%, Dumesic's group reported that a high HMF yield of 97% could be achieved in a mixture of acetone and water (entry 7).[35] However, very low substrate concentration inevitably means the utilization of a large amount of solvent, which substantially diminishes the potential for large-scale employment. When the fructose loading was increased to 30 wt%, a rather complex solvent mixture of water and methylisobutylketone (MIBK) with additives of DMSO, poly(1-vinyl-2-pyrrolidinone) (PVP), and 2-butanol resulted in a 73% HMF yield (entry 8).[36] This system was later simplified by using a mixture of saturated NaCl aqueous solution and 1-butanol; however, the HMF yield (66%) was lower (entry 9).[3] More recently, a microwave-assisted biphasic mixture of aqueous KBr and acetonitrile produced a decent HMF yield (85%) from fructose dehydration; however, the fructose concentration (10 wt%) was still quite low.[37]

These aforementioned accomplishments would naturally result in an impression that these technologies should already be adopted in industry; however, this has not yet been realized. The appealing synthetic promise of HMF results from its three functional moieties: a furan ring, a hydroxymethyl group, and an aldehyde. The reactivity of HMF in the syntheses of valuable products is also the very reason for its susceptibility towards hydrolysis and other side reactions during its own synthesis from carbohydrates (*e.g.*, fructose). Prolonged storage of HMF in its oily state will lead to rapid and irreversible oligo polymerization into insoluble humins. Besides poor chemical stability, the large-scale production of HMF also suffers from its challenging isolation and purification from reaction mixtures. Distillation is not an ideal option, as elevated temperature will facilitate the undesirable formation of humins. Overall, the limited stability and difficult isolation of HMF severely undermine its potential for large-scale synthetic purposes. It should be noted that in most of the fructose dehydration studies reported previously, the HMF yields were determined *via* HPLC or GC. Isolated HMF yield has rarely been reported, most likely due to the challenges in its isolation and purification as well as the low concentration of fructose usually utilized. As shown in Fig. 1a, even though HMF is regarded as a biomass-derived platform chemical, its own production has become the bottleneck for the syntheses of valuable chemicals because of its poor stability and difficult isolation. In order to overcome these obstacles, we reason that it is very appealing to synthesize value-added products directly from fructose without the separation of HMF in the middle of the entire process,

Table 1 A summary of the representative conditions and yields for the conversion of fructose to HMF

Entry	Catalyst	Solvent	Con. (wt%)	T (°C)	Time (min)	Yield (%)	Ref.
1	HCl	H_2O	27	200[a]	1	53	30
2	H_2SO_4	DMA + NaBr	10	100	240	92	31
3	H_2SO_4	DMSO	16	100	300	93	32
4	H_2SO_4	HCOOH	16	150	120	73	32
5	HCl	GVL + H_2O	15	180	30	70	33
6	HCl	GVL + H_2O	1	100	60	78	34
7	HCl	Acetone + H_2O	1	120	30	97	35
8	HCl	H_2O + DMSO + PVP + MIBK + 2-butanol	30	180	3	73	36
9	HCl	NaCl (aq.) + 1-butanol	30	180	3	66	3
10	HCl	KBr (aq.) + MeCN	10	160[a]	1	85	37

[a] Under microwave irradiation.

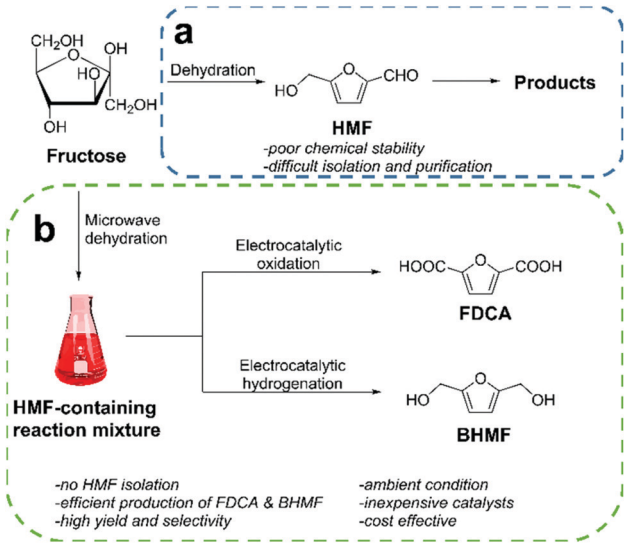

Fig. 1 (a) Conventional strategies for the syntheses of value-added products from carbohydrates (*e.g.*, fructose), with HMF produced as a key intermediate. (b) Our approach for the direct production of FDCA and BHMF from fructose without the isolation of HMF.

which should significantly simplify the overall route and reduce cost.

Herein, we report an innovative strategy for the syntheses of FDCA and BHMF from fructose, taking the advantages of microwave-assisted fructose dehydration and electrocatalytic conversion of HMF in the reaction mixture under ambient conditions (Fig. 1b). A biphasic solvent system compatible with the subsequent electrocatalysis was adopted to perform fructose dehydration under microwave irradiation, and an HMF yield of 83% was obtained even when a very high fructose concentration (100 wt%) was utilized. The resulting microwave reaction mixture could be used for either electrocatalytic oxidation or electrocatalytic hydrogenation to produce FDCA or BHMF, respectively, under appropriate conditions. Nearly quantitative yields of FDCA and BHMF, together with high faradaic efficiency, were obtained. Long-term electrolysis in a flow-cell electrolyzer was also employed to demonstrate the practical potential of our strategy for large-scale application.

2. Experimental section

2.1 Chemicals and reagents

The following chemicals were purchased and used as received: fructose, 5-hydroxymethylfurfural (HMF) and 2,5-furandicarboxylic acid (FDCA) were purchased from J&K Scientific, Alfa Aesar, and Chem-Impex, respectively. $AgNO_3$, $NiCl_2{\cdot}6H_2O$ and NaOH were purchased from Fisher Scientific. Nickel and copper foam with >99.99% purity were purchased from MTI. Deionized water (18 MΩ cm) from a Barnstead E-Pure system was used in all experiments. All the other reagents and solvents were purchased from commercial sources and used without purification.

2.2 Fructose dehydration under microwave irradiation

To a 40 mL microwave vessel with a magnetic stir bar and containing fructose (1.5 g) was added 1.5 mL saturated NaCl aqueous solution containing 70 μL (10 mol% *vs.* fructose) HCl. Then, 3 mL THF was added to the vessel, and the biphasic mixture was subjected to microwave irradiation (CEM Discover) for a certain period of time. With the microwave irradiation power of 150 W, it took ~45 s to reach 140 °C. After a certain period of reaction time, the vessel was cooled down to room temperature immediately. Subsequently, the rection mixture was diluted with DI water for further HPLC analysis or electrolysis.

The weight percentage of fructose was calculated based on the following equation,[35–37]

$$\text{Weight percentage}\,(wt\%) = \frac{\text{mass of solute}}{\text{mass of solvent}\,(H_2O)} \times 100\%\ .$$

2.3 Preparation of electrodes

Ni/NF was prepared by cathodic electrodeposition of nickel particles on nickel foam. The electrodeposition was carried out with a two-electrode configuration in a cell containing 50 mL NH_4Cl (2.0 M) and $NiCl_2$ (0.1 M) at room temperature. A piece of clean nickel foam (1 × 3 cm^2) and a carbon rod were used as the working and counter electrodes, respectively. The electrodeposition was performed at a constant current of −0.4 A for 0.5 h under N_2 protection without stirring. Ag/Cu was prepared by dipping copper foam (1 × 3 cm^2) into 1 mM $AgNO_3$ solution for 12 h and washing with water.

2.4 Electrochemical measurements for batch electrolysis

Electrochemical measurements were performed using a BioLogic potentiostat in a three-electrode configuration. The as-prepared Ni/NF (or Ag/Cu) was directly used as the working electrode, a saturated calomel (sat. KCl) electrode as the reference electrode, and a carbon rod as the counter electrode. The experiments were conducted in 10 mL electrolyte with and without organic substrate in an H-cell.

2.5 Electrolysis in continuous flow mode

Three pieces of Ni/NF (or Ag/Cu) (1 × 3 cm^2) were compressed and used as the working and counter electrodes. Working and counter chambers were separated by an anion exchange membrane (Fumapem FAA-3-50). Electrolyte for the electrocatalytic hydrogenation of HMF was bubbled with N_2 for 15 min prior to utilization. Flow rates were controlled by peristaltic pumps from Miniature (BQ50-1J-J) and Karmoer (KCP3-B08 W).

2.6 Product quantification

During electrolysis, 10 μL of each electrolyte solution was withdrawn and diluted with 990 μL water, then analyzed at 25 °C using a Hitachi infinity 1050 HPLC system equipped with an ultraviolet–visible detector and a 4.6 mm × 150 mm Shim-pack GWS 5 μm C18 column. A mixture of eluting solvents (A and B) was utilized. Solvent A was 5 mM ammonium acetate aqueous solution, and solvent B was methanol. Separation and quantifi-

cation were accomplished using an isocratic elution of 60% A and 40% B for 5 min run time, and the flow rate was set at 0.5 mL min^{-1} for the quantification of HMF and FDCA. Separation and quantification were accomplished using an isocratic elution of 85% A and 15% B for 15 min run time, and the flow rate was set at 0.5 mL min^{-1} for the quantification of HMF and BHMF. The identification and quantification of each compound were determined from the calibration curve by applying standard solutions with known concentrations of the commercially purchased pure sample. The retention and conversion (%) of HMF and the yield (%) of products were calculated based on the following equations:

$$\text{Retention}\ (\%) = \frac{\text{mole of substrate after reaction}}{\text{mole of initial substrate}} \times 100\%$$

$$\text{Conversion}\ (\%) = \frac{\text{mole of substrate consumed}}{\text{mole of initial substrate}} \times 100\%$$

$$\text{Yield}\ (\%) = \frac{\text{mole of product formed}}{\text{mole of initial substrate}} \times 100\%\ .$$

The faradaic efficiency (FE) of product formation was calculated using the following equation:

$$\text{FE}\ (\%) = \frac{\text{mole of product formed}}{\text{total charge passed}/(n \times F)} \times 100\%\ ,$$

where n is the number of electrons transferred for each product formation, and F is the Faraday constant (96 485 C mol^{-1}).

2.7 Gram-scale synthesis of FDCA and BHMF

The biphasic solution after fructose dehydration reaction was diluted with DI water to a homogeneous solution containing 50 mM fructose-derived HMF. For HMF oxidation, NaOH was added to the above solution until it reached 1.0 M, which was used as the electrolyte. For HMF hydrogenation, a solution containing 30 mM fructose-derived HMF in 0.5 M borate buffer was prepared in the same way. Three pieces of Ni/NF (or Ag/Cu) (4 × 7 cm^2) were compressed and used as the working electrodes. Electrolyte for the electrocatalytic HMF hydrogenation was bubbled with N_2 throughout the electrolysis. The applied current was 400 and −40 mA at flow rates of 15 and 5 mL h^{-1} for electrocatalytic HMF oxidation and hydrogenation, respectively.

2.8 Post-processing during the gram-scale synthesis of FDCA and BHMF

To a 250 mL outlet solution of electrocatalytic HMF oxidation was added hydrochloric acid to pH 3, and the solvent was removed under vacuum. 350 mL *n*-butanol was added to the resulting solid and stirred for 0.5 h. The mixture was filtered, and the filtrate was dried under vacuum. The thus obtained solid phase was washed with a small amount of acetone to yield FDCA as a white solid. The outlet solution of electrocatalytic HMF hydrogenation was extracted with ethyl acetate and dried under vacuum. BHMF was obtained *via* recrystallization in methanol and diethyl ether.

3. Results and discussion

3.1 Microwave-assisted fructose dehydration

Different from conventional heating methods, microwave irradiation more effectively provides kinetic energy input to substrates and results in simultaneous and even temperature increase throughout the reaction medium and, hence, shorter reaction time and less side reactions.[38] As such, microwave irradiation has been widely recognized as a green synthetic approach that has been successfully applied not only in laboratories but also in industry.[39,40] In order to design a synthetic route for the conversion of fructose to FDCA (or BHMF) directly without the isolation of HMF, it is essential that the solvent system adopted for the microwave-assisted fructose dehydration be compatible with the subsequent electrochemical step(s). Consequently, the reported organic solvents (*e.g.*, acetone and 1-butanol) and additives (*e.g.*, Br- and formic acid) are no longer appropriate. Furthermore, in order to simplify the separation of final products, organic solvents with high boiling points, such as DMSO and DMA, are better avoided. With these considerations and a thorough literature study in mind, we proposed a biphasic solvent system consisting of saturated NaCl aqueous solution and THF for fructose dehydration under microwave irradiation.[37,41] Even though water and THF are miscible, the very high concentration of NaCl in water makes it immiscible with THF due to the salting out effect. Such a biphasic solvent system favours the migration of HMF from the aqueous phase to the organic phase, therefore diminishing HMF rehydration. In addition, the presence of Cl^- is able to stabilize the intermediates of fructose dehydration and thus suppress the formation of side products from polycondensation.[31]

Specifically, microwave-assisted fructose dehydration was performed at 140 °C with 10 mol% (*vs.* fructose) HCl as the catalyst. A representative image of the reaction vial post-microwave treatment, shown in Fig. S1,† clearly presents two distinctive layers, confirming the separation of the organic phase (top layer) from the aqueous phase, wherein the much darker colour of the organic phase implied the favourable distribution of HMF (and other organic side products) in the top layer. With the aim of large-scale application, high fructose concentration and fast reaction time are very much preferred. Therefore, we systematically optimized the starting concentration of fructose and the duration of microwave irradiation. The final HMF yields were quantified *via* HPLC. As summarized in Fig. 2 and Table S1,† fructose concentration was varied from 20 wt% to an unprecedentedly high 200 wt%, and the microwave treatment was increased from 0.1 to 2 min. The highest HMF yield of 83% was obtained with 100 wt% fructose concentration and merely 1 min of microwave treatment. It should be noted that even the 200 wt% loading of fructose was also able to produce HMF with a yield of 73% within 0.5 min of microwave irradiation. Such a high fructose starting concentration, together with a decent HMF yield, has never been reported before (Table 1), strongly suggesting the promise of

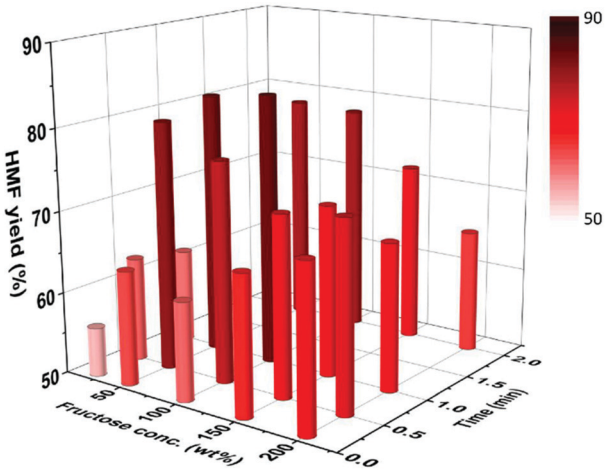

Fig. 2 HMF yields from microwave-assisted fructose dehydration with varying fructose starting concentrations and microwave irradiation durations.

our microwave-assisted biphasic solvent system for the practical dehydration of fructose on a large scale.

3.2 Electrooxidation of fructose-derived HMF in a batch electrolyzer

Even though electrochemical oxidation of HMF to yield FDCA and other oxidized products has been extensively studied these years, all the HMF used are purchased commercially, with high purity (>95%). There have been no reports on the direct electrosynthesis of FDCA from the reaction mixture of fructose dehydration. Herein, we decided to carry out the electrochemical study of fructose dehydration solution with nickel foam (NF) decorated with electrodeposited nickel nanoparticles (Ni/NF) as the working electrode, since our previous work demonstrated the superior effectiveness of Ni/NF for the electrooxidation of pure HMF to produce FDCA under alkaline conditions.[16–18] As a comparison, cyclic voltammogram of Ni/NF was also collected in blank 1.0 M NaOH. A distinctive $Ni^{III/II}$ redox feature was observed in the potential range of 0.2 and 0.7 V *vs.* SCE. Beyond 0.7 V *vs.* SCE, an anticipated current rise due to the O_2 evolution reaction (OER) was confirmed (Fig. 3a). Subsequently, electrochemical study of our fructose-derived HMF was performed. Since the as-obtained HMF solution after fructose dehydration was still biphasic, it was diluted with DI water to prepare a homogeneous solution containing 10 mM fructose-derived HMF. Afterwards, solid NaOH was added to reach 1.0 M NaOH solution, which was used as the electrolyte. A substantially higher current was observed after the $Ni^{III/II}$ anodic peak compared to that in blank 1.0 M NaOH solution, implying the oxidation of HMF and/or other remnants from the microwave irradiation reaction. A plateau was observed in the range of 0.62 and 0.72 V *vs.* SCE. In order to achieve high faradaic efficiency, long-term electrolysis was performed at 0.7 V *vs.* SCE, prior to the OER onset. Fig. S2† shows the decreasing chronoamperometric curve and the

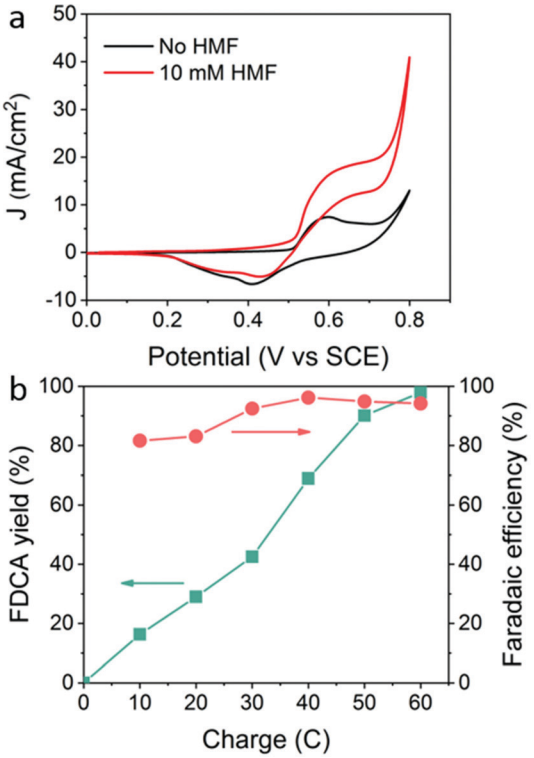

Fig. 3 (a) Cyclic voltammograms of Ni/NF in blank 1.0 M NaOH (black) and 1.0 M NaOH containing 10 mM fructose-derived HMF (red) (scan rate = 10 mV s^{-1}). (b) Evolution of the FDCA yield and the corresponding faradaic efficiency during electrolysis in a batch electrolyzer at an applied potential of 0.7 V *vs.* SCE.

accumulation of passed charge during electrolysis. The rate of charge accumulation decreased with the decreasing current. This observation is consistent with the consumption of HMF in the electrolyte. HPLC was utilized to quantify the amount of produced FDCA, and the faradaic efficiency was also calculated (Fig. S3†). After passing the charge of 60 C, nearly 100% yield was achieved for FDCA formation together with a faradaic efficiency of 96% (Fig. 3b). It should be noted that the calculated faradaic efficiency remained as high as >80% during the entire course of electrolysis, suggesting no appreciable interference of OER. More importantly, the very high FDCA yield and its faradaic efficiency also confirmed that the presence of any residual chemicals like THF, Cl^-, and other potential side products from the microwave-assisted fructose dehydration did not affect the electrooxidation of HMF to FDCA in our system.

3.3 Electrooxidation of fructose-derived HMF in a flow electrolyzer

The aforementioned results obtained in a batch electrolyzer unambiguously proved the feasibility of our strategy in fructose conversion to FDCA. Nevertheless, the decreased current due to the substrate consumption in a batch electrolyzer will undoubtedly lead to long electrolysis time and low efficiency. With the aim of practical application, we next sought to

conduct the electrooxidation in a flow electrolyzer (Fig. S4†). In fact, flow electrolysis has witnessed great success for many organic reactions, not only on a lab scale but also in industry.[42–48]

Prior to utilizing the microwave reaction mixture after fructose dehydration for flow electrolysis, we first used pure HMF to optimize the electrolysis conditions. As plotted in Fig. 4a, the cyclic voltammograms of Ni/NF collected in a two-electrode configuration also presented a $Ni^{III/II}$ redox feature in 1.0 M NaOH. Once 20 mM HMF was added to the flow electrolyte, an anodic current increase was observed when the applied voltage on Ni/NF was larger than 1.5 V, and a maximum current density of 10 mA cm^{-2} was obtained at 1.65 V before the OER onset. In order to study the relationship between catalytic rate and HMF concentration, a series of CV curves were collected with different HMF concentrations (Fig. S5†). Fig. S4b† clearly showed the increased maximum current density with increasing HMF concentration in a relatively low concentration range. However, a plateau was observed when the HMF concentration was higher than 4 mM. Electrolyte flow rate is another crucial factor in controlling electrolysis efficiency. Fig. 4c shows the dependence of current maximum on the electrolyte flow rate when five different electrolytes, containing 1, 2, 4, 6, and 8 mM HMF, were tested. Different from those electrolytes with very low HMF concentration (like 1 mM), once the HMF concentration was larger than 6 mM, no significant current increase was observed along the increase of electrolyte flow rate in our flow electrolyzer setting (Fig. 4c and S6†). A series of long-term electrolyses was conducted at different applied voltages, ranging from 1.4 to 1.8 V. Fig. 4d shows the chronoamperometric curves for 20 mM HMF oxidation in 1.0 M NaOH with an electrolyte flow rate of 5 mL h^{-1}. The fluctuation of the chronoamperometric curves obtained at 1.7 and 1.8 V was likely due to the formation and release of O_2 bubbles on Ni/NF. In striking contrast to the decreasing chronoamperometric curves over time in batch electrolysis (Fig. S2†), flow electrolysis presented very stable current at all the applied voltages and, hence, linearly increasing accumulation of passed charge (Fig. 5e). The concentrations of residual HMF and produced FDCA in the outlet electrolyte flow were quantified *via* HPLC (Fig. S7†). Fig. 4f summarizes the results of flow electrolysis at different applied voltages. When the applied voltage was as low as 1.4 V on Ni/NF, a unity faradaic efficiency was obtained for FDCA formation, albeit its yield was only 20%. Along with the increase of applied voltage, a substantial increase in FDCA yield was achieved with a slightly decreasing faradaic efficiency. The optimal result was obtained at 1.7 V, where both FDCA yield and the corresponding faradaic efficiency were above 90%. Further increasing the applied voltage to 1.8 V would result in severe interference of OER and hence a low faradaic efficiency (47%); nevertheless, the FDCA yield was still as high as 97%. With an increase of the working electrode area from 3 to 28 cm^2, an improved faradaic

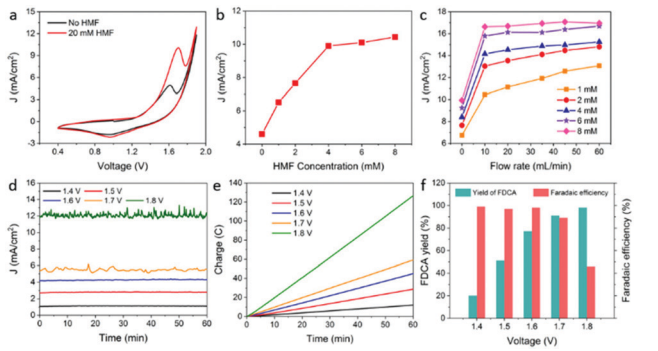

Fig. 4 (a) Cyclic voltammograms of Ni/NF before and after the addition of 20 mM HMF in 1.0 M NaOH using a two-compartment flow cell (scan rate = 10 mV s^{-1}). (b) Dependence of the current density maximum with varying HMF concentrations in 1.0 M NaOH. (c) Dependence of the current density maximum with varying HMF concentrations on the flow rate of the electrolyte. (d) Chronoamperometric and (e) charge accumulation curves from the electrooxidation of 20 mM HMF in 1.0 M NaOH using a flow electrolyzer with different applied voltages (flow rate = 5 mL h^{-1}). (f) Dependence of the FDCA yield and its corresponding faradaic efficiency on the applied voltage during flow electrolysis.

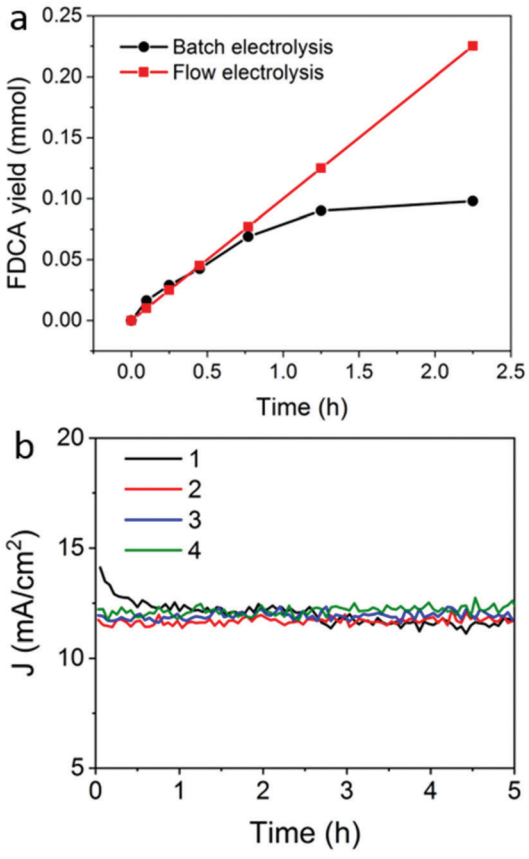

Fig. 5 (a) FDCA yield over time during electrolysis, using either a batch electrolyzer (black) or a flow electrolyzer (red). (b) Chronoamperometric curves from the electrooxidation of the microwave reaction mixture of fructose dehydration in 1.0 M NaOH using the same Ni/NF working electrode for four consecutive flow electrolysis cycles. The HMF concentration was measured at 20 mM in the electrolyte, and the applied voltage was 1.8 V.

efficiency of 92% could be achieved at 1.5 V, while a 95% FDCA yield was maintained, owing to less competing OER activity at lower potentials compared to that with a small electrode at 1.7 V (Fig. S8†).

After the above study on electrooxidation of HMF in a flow electrolyzer, we next performed electrolysis using the reaction mixture after the microwave-assisted dehydration of fructose in 1.0 M NaOH. As shown in Fig. S9,† no HMF was detected in the outlet electrolyte when the electrolysis was conducted at 1.8 V, and a 96% yield was measured for FDCA, which was comparable to the results of batch electrolysis. However, the advantage of flow electrolysis was manifested in the linearly increased amount of produced FDCA, while the yield from a batch electrolyzer was limited by the original HMF concentration. As demonstrated in Fig. 5a, a flow electrolyzer already produced two times more FDCA than a batch electrolyzer within 2.5 h electrolysis in our systems. Four consecutive electrolysis cycles using the same Ni/NF electrode resulted in identical current density (Fig. 5b), which illustrates the excellent robustness of our flow electrolysis system and its strong resistance towards those additives and impurities from the pre-step of fructose dehydration. To further demonstrate the scalability of the FDCA production using this flow electrolyzer, the gram-scale production of FDCA was also carried out. Starting with 2.5 g fructose, our two-step process could produce 1.7 g isolated FDCA with an overall yield of 76%. Fig. S10† shows a photograph of FDCA as a white solid, and its ^{1}H and ^{13}C NMR spectra are included in Fig. S11 and S12,† respectively.

3.4 Electrocatalytic hydrogenation of fructose-derived HMF in a flow electrolyzer

Our strategy in converting fructose to value-added products is not limited to the production of FDCA *via* electrochemical oxidation. Instead, owing to the flexible tunability of electrocatalysis, it is equally feasible to conduct electrocatalytic hydrogenation of the resulting microwave reaction mixture in aqueous electrolyte to yield another valuable biopolymer precursor, BHMF.

A porous copper foam was immersed in a 1 mM $AgNO_3$ solution for 12 h to galvanically deposit a silver layer on copper. The resulting Ag/Cu foam was used as the working electrode for the electrocatalytic hydrogenation. Similar to the above electrooxidation, electrocatalytic hydrogenation was first performed in a three-electrode configuration. As shown in Fig. S13,† the linear sweep voltammogram (LSV) of Ag/Cu collected in a pristine borate buffer at pH 9 presented a cathodic current take-off beyond −1.0 V *vs.* SCE, most likely due to H_2 evolution (HER). The electrolyte of 0.5 M borate buffer containing 10 mM fructose-derived HMF was prepared by adding boric acid and NaOH into the diluted solution of fructose dehydration. A substantial anodic shift of the LSV curve was observed with a new onset potential at −0.85 V *vs.* SCE in the electrolyte containing fructose-derived HMF. A current plateau between −0.96 and −1.05 *vs.* SCE was attributed to the limited mass diffusion of HMF in the electrolyte, followed by a rapid cathodic current rise of HER beyond −1.1 *vs.* SCE. A similar trend of HMF being reduced at more positive potential than H_2O was also observed in a flow electrolyzer (Fig. 6a). Subsequently, long-term electrolysis in a two-electrode configuration was carried out using a flow electrolyzer, as described above for electrooxidation. The only difference was that the working electrode was Ag/Cu. Fig. 6b presents the HMF retention and BHMF yield for three flow electrolysis experiments conducted at different applied voltages, −1.5, −1.7, and −1.9 V. It is apparent that best result was obtained with a voltage input of −1.9 V, which led to nearly zero HMF retention, while a very high BHMF yield of 97% was achieved. The concentrations of HMF and BHMF in the outlet flow of the electrolyte during flow electrolysis were both quantified *via* HPLC (Fig. S14†). In addition, two consecutive flow electrolysis set-ups using the same flow electrolysis setting but with different microwave reaction mixtures showed perfectly overlapped HPLC traces (Fig. S15†), confirming the reproducibility of our flow cell system for the electrocatalytic hydrogenation of fructose dehydration mixture to synthesize BHMF directly. Gram-scale production of BHMF from fructose-derived HMF was obtained with an isolated yield of 72% (1.2 g) starting from fructose, highlighting the promise of our strategy for large-scale synthesis. The corresponding ^{1}H and ^{13}C NMR

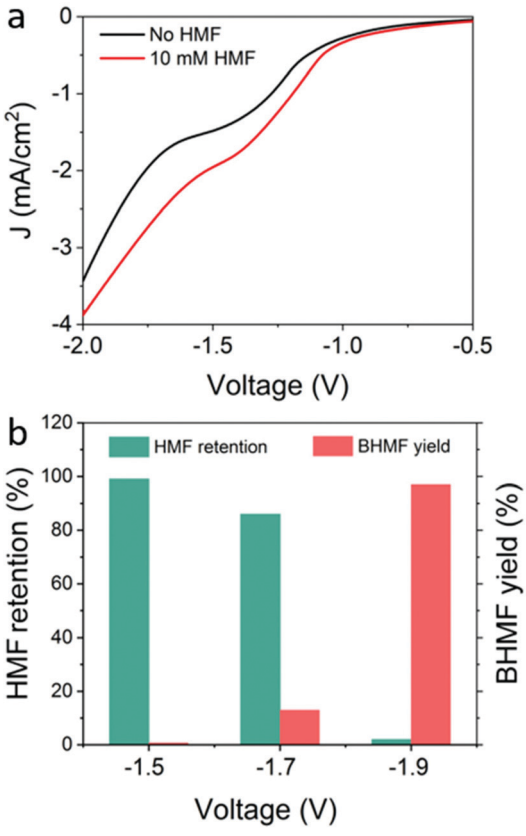

Fig. 6 (a) LSV curves collected on a Ag/Cu electrode in blank 0.5 M borate buffer (pH 9.0) (black) and in 0.5 M borate buffer containing 10 mM fructose-derived HMF (red) (scan rate = 10 mV s^{-1}). (b) HMF retention and BHMF yield from flow electrolysis performed at different applied voltages.

spectra of the synthesized BHMF are shown in Fig. S16 and S17.†

4. Conclusions

In summary, an innovative strategy has been developed for the direct synthesis of value-added biopolymer precursors (*e.g.*, FDCA and BHMF) from fructose. Troublesome and high-cost HMF isolation as an intermediate step is completely avoided. Given the unique advantages of microwave-assisted biphasic dehydration, integrated with electrocatalytic transformation for both oxidation and hydrogenation, we achieved superior results for the overall process, including a high HMF yield from unprecedentedly concentrated fructose solution (up to 200 wt%) within minutes and great yields of FDCA and BHMF, as well as excellent faradaic efficiency. Such a modular strategy is very convenient for modification to meet the requirements of many other reaction sequences if a challenging intermediate step needs to be bypassed; thus, it presents great potential for much broader applications beyond biomass valorisation.

Conflicts of interest

There are no conflicts to declare.

Acknowledgements

Y. S. acknowledges financial support from the National Science Foundation (CHE-1914546) and the University of Cincinnati. NMR experiments were performed using a Bruker AVANCE NEO 400 MHz NMR spectrometer (funded by NSF-MRI grant CHE-1726092).

Notes and references

1 A. Corma, S. Iborra and A. Velty, *Chem. Rev.*, 2007, **107**, 2411–2502.
2 C.-J. Li and B. M. Trost, *Proc. Natl. Acad. Sci. U. S. A.*, 2008, **105**, 13197–13202.
3 Y. Román-Leshkov, C. J. Barrett, Z. Y. Liu and J. A. Dumesic, *Nature*, 2007, **447**, 982–985.
4 R.-J. van Putten, J. C. van der Waal, E. de Jong, C. B. Rasrendra, H. J. Heeres and J. G. de Vries, *Chem. Rev.*, 2013, **113**, 1499–1597.
5 I. Delidovich, P. J. C. Hausoul, L. Deng, R. Pfützenreuter, M. Rose and R. Palkovits, *Chem. Rev.*, 2016, **116**, 1540–1599.
6 W. J. Pentz, *U.S. Patent*, 19840117, 1984.
7 W. R. Dunlop and W. J. Pentz, *U.S. Patent*, 19820309, 1982.
8 R. J. I. Knoop, W. Vogelzang, J. van Haveren and D. S. van Es, *J. Polym. Sci., Part A: Polym. Chem.*, 2013, **51**, 4191–4199.
9 S. K. Burgess, J. E. Leisen, B. E. Kraftschik, C. R. Mubarak, R. M. Kriegel and W. J. Koros, *Macromolecules*, 2014, **47**, 1383–1391.
10 S. K. Burgess, O. Karvan, J. R. Johnson, R. M. Kriegel and W. J. Koros, *Polymer*, 2014, **55**, 4748–4756.
11 M. L. Ribeiro and U. Schuchardt, *Catal. Commun.*, 2003, **4**, 83–86.
12 N. K. Gupta, S. Nishimura, A. Takagaki and K. Ebitani, *Green Chem.*, 2011, **13**, 824–827.
13 J. C. van der Waal, E. Mazoyer, H. J. Baars and G.-J. M. Gruter, *Liquid phase aerobic oxidation catalysis: industrial applications and academic perspectives*, Wiley-VCH Verlag GmbH & Co. KGaA, 2016, pp. 311–329.
14 T. Pasini, M. Piccinini, M. Blosi, R. Bonelli, S. Albonetti, N. Dimitratos, J. A. Lopez-Sanchez, M. Sankar, Q. He and C. J. Kiely, *Green Chem.*, 2011, **13**, 2091–2099.
15 S. E. Davis, B. N. Zope and R. J. Davis, *Green Chem.*, 2012, **14**, 143–147.
16 B. You, N. Jiang, X. Liu and Y. Sun, *Angew. Chem., Int. Ed.*, 2016, **55**, 9913–9917.
17 B. You, X. Liu, N. Jiang and Y. Sun, *J. Am. Chem. Soc.*, 2016, **138**, 13639–13646.
18 B. You, X. Liu, X. Liu and Y. Sun, *ACS Catal.*, 2017, **7**, 4564–4570.
19 Y. Nakagawa and K. Tomishige, *Catal. Commun.*, 2010, **12**, 154–156.
20 R. Alamillo, M. Tucker, M. Chia, Y. Pagán-Torres and J. Dumesic, *Green Chem.*, 2012, **14**, 1413–1419.
21 X. Liu, B. You and Y. Sun, *ACS Sustainable Chem. Eng.*, 2017, **5**, 4778–4784.
22 B. You, X. Liu, G. Hu, S. Gul, J. Yano, D. Jiang and Y. Sun, *J. Am. Chem. Soc.*, 2017, **139**, 12283–12290.
23 X. Liu, J. Chi, B. Dong and Y. Sun, *ChemElectroChem*, 2019, **6**, 2157–2166.
24 E. Kirowa-Eisner and E. Gileadi, *J. Electroanal. Chem. Interfacial Electrochem.*, 1972, **38**, 191–201.
25 W. R. Fawcett and A. Lasia, *Can. J. Chem.*, 1981, **59**, 3256–3260.
26 Y. Kwon and M. T. M. Koper, *ChemSusChem*, 2013, **6**, 455–462.
27 Y. Kwon, Y. Y. Birdja, S. Raoufmoghaddam and M. T. M. Koper, *ChemSusChem*, 2015, **8**, 1745–1751.
28 P. Nilges and U. Schröder, *Energy Environ. Sci.*, 2013, **6**, 2925–2931.
29 J. J. Roylance, T. W. Kim and K.-S. Choi, *ACS Catal.*, 2016, **6**, 1840–1847.
30 T. S. Hansen, J. M. Woodley and A. Riisager, *Carbohydr. Res.*, 2009, **344**, 2568–2572.
31 J. B. Binder and R. T. Raines, *J. Am. Chem. Soc.*, 2009, **131**, 1979–1985.
32 T. Thananatthanachon and T. B. Rauchfuss, *Angew. Chem., Int. Ed.*, 2010, **49**, 6616–6618.
33 A. H. Motagamwala, W. Won, C. Sener, D. M. Alonso, C. T. Maravelias and J. A. Dumesic, *Sci. Adv.*, 2018, **4**, eaap9722.

34 M. A. Mellmer, C. Sanpitakseree, B. Demir, K. Ma, W. A. Elliott, P. Bai, R. L. Johnson, T. W. Walker, B. H. Shanks and R. M. Rioux, *Nat. Commun.*, 2019, **10**, 1132.
35 A. H. Motagamwala, K. Huang, C. T. Maravelias and J. A. Dumesic, *Energy Environ. Sci.*, 2019, **12**, 2212–2222.
36 Y. Roman-Leshkov, *Science*, 2006, **312**, 1933–1937.
37 P. Wrigstedt, J. Keskiväli and T. Repo, *RSC Adv.*, 2016, **6**, 18973–18979.
38 R. Morschhäuser, M. Krull, C. Kayser, C. Boberski, R. Bierbaum, P. A. Püschner, T. N. Glasnov and C. O. Kappe, *Green Process. Synth.*, 2012, **1**, 281–290.
39 S. Dąbrowska, T. Chudoba, J. Wojnarowicz and W. Łojkowski, *Crystals*, 2018, **8**, 379.
40 R. Nagahata and K. Takeuchi, *Chem. Rec.*, 2019, **19**, 51–64.
41 F. Delbecq and C. Len, *Molecules*, 2018, **23**, 1973.
42 J. Yoshida, *Flash Chemistry: Fast Organic Synthesis in Microsystems*, Wiley-VCH, Weinheim, Germany, 2008.
43 S. V. Luis and E. Garcia-Verdugo, *Chemical Reactions and Processes under Flow Conditions*, Royal Society of Chemistry, Cambridge, U.K, 2009.
44 T. Wirth, *Microreactors in Organic Synthesis and Catalysis*, Wiley-VCH, Weinheim, Germany, 2nd edn, 2008.
45 W. Reschetilowski, *Microreactors in Preparative Chemistry*, Wiley-VCH, Weinheim, Germany, 2013.
46 M. Atobe, H. Tateno and Y. Matsumura, *Chem. Rev.*, 2018, **118**, 4541–4572.
47 D. Pletcher, R. A. Green and R. C. D. Brown, *Chem. Rev.*, 2018, **118**, 4573–4591.
48 D. Wang, P. Wang, S. Wang, Y.-H. Chen, H. Zhang and A. Lei, *Nat. Commun.*, 2019, **10**, 2796.